33RD INTERNATIONAL COSMIC RAY CONFERENCE, RIO DE JANEIRO 2013
THE ASTROPARTICLE PHYSICS CONFERENCE

ICRC 2013

Multipole analysis with IceCube to search for dark matter accumulated in the Galactic Halo

THE ICECUBE COLLABORATION[1],

[1] *See special section in these proceedings*

reimann@physik.rwth-aachen.de

Abstract: Self-annihilating or decaying dark matter in the Galactic Halo may contribute to the observed flux of cosmic particles, e.g. gammas, positrons or neutrinos. High-energy neutrinos can be detected with the IceCube Neutrino Observatory, a cubic-kilometer-sized Cherenkov detector at the geographical South Pole. The additional flux from dark matter annihilation depends on the density of dark matter in the direction of sight and is expected to be larger in the direction of the galactic center and smaller in the direction of the anti-center. Given the large field of view of IceCube, such a large-scale anisotropy would leave a characteristic imprint on multipole expansion coefficients of the observed set of arrival directions in a high-purity muon neutrino event sample that can be obtained by selecting up-going muon events. This imprint can be interpreted in terms of the thermally averaged self-annihilation cross-section of dark-matter particles. We discuss the analysis of IceCube data in the 79-string configuration, using neutrinos from the Northern hemisphere. This analysis improves in sensitivity with respect to previous IceCube analyses. Resulting exclusion limits on the velocity averaged annihilation cross-section are presented.

Corresponding authors: René Reimann[1],
[1] *III. Physikalisches Institut, RWTH Aachen University, D-52056 Aachen, Germany*

Keywords: Dark Matter, Galactic Halo, IceCube

1 Introduction

A variety of astronomical observations imply the existence of non-baryonic cold dark matter in the Universe. The velocity distribution of galaxy clusters suggests a mass content significantly higher than what should be expected from observations of the luminous mass [1]. Also the rotation profiles of galaxies show discrepancies to the expectation that hint at the existence of a dark matter halo reaching out far beyond the baryonic disc and bulge [1]. Based on, e.g., the anisotropy in the cosmic microwave background observed by the Wilkinson Microwave Anisotropy Probe [2] or Planck [3], a determination of cosmological parameters is possible, which yields the concordance model of cosmology with a dark matter content of about 22%. Large-scale structure formation and N-body simulations favor cold dark matter that consists of massive and non-relativistic particles. Weakly Interacting Massive Particles (WIMPs) are the generic candidates for cold dark matter in a mass range from a few GeV up to several 100 TeV [4, 5]. A promising WIMP candidate is the lightest stable particle in minimal super-symmetric extension to Standard Model.

If WIMPs are Majorana particles, they can self-annihilate and produce Standard Model particles in the final state. Observable stable messenger particles (e.g. photons, neutrinos, charged cosmic rays), could be produced as annihilation products, or in their decays. Since dark matter particles may be bound in the Galactic Halo, we expect this excess flux of neutral particles from self-annihilations to display a large-scale anisotropy that should map the dark matter density distribution in the galaxy. Due to the shape of the halo, this flux should be stronger towards the central part of our galaxy.

2 Neutrino flux from dark matter annihilation in the Galactic Halo

Predicted dark matter density profiles are based on observations of dark-matter-dominated galaxies and simulations of N-body systems [6]. An often used parametrization of a spherically symmetric dark-matter density profile is

$$\rho_{\mathrm{DM}}(r) = \frac{\rho_0}{\left(\frac{r}{r_s}\right)^{\gamma} \cdot \left[1+\left(\frac{r}{r_s}\right)^{\alpha}\right]^{(\beta-\gamma)/\alpha}}, \qquad (1)$$

where r is the distance from the Galactic Center (GC) in kpc and r_s is a scaling radius [7]. Commonly, the Navarro-Frenk-White (NFW) profile with the parameters $r_s = 20\,\mathrm{kpc}$ and $(\alpha,\beta,\gamma) = (1,3,1)$ [8] is used. ρ_0 is chosen such that the local dark-matter density at the radius of the solar circle R_{SC} is $0.3\,\mathrm{GeV/cm^3}$. Other common models are e.g. the Moore profile [9] or the Burkert profile [10].

The flux from self-annihilating dark matter depends on the density squared along the line of sight

$$J_a(\psi) = \int_0^{l_{max}} \mathrm{d}l \frac{\rho^2_{\mathrm{DM}}\left(\sqrt{R^2_{\mathrm{SC}} - 2lR_{\mathrm{SC}}\cos\psi + l^2}\right)}{R_{\mathrm{SC}}\rho^2_{\mathrm{SC}}}, \qquad (2)$$

where ψ is the opening angle between the line of sight and the GC [11]. R_{SC} and ρ^2_{SC} are constants for scaling and l_{max} is approximately the radius of the Milky Way. The line-of-sight integral for the Northern hemisphere is shown in Fig. 1. The flux is large in the direction of the galactic center and small in the direction of the anti-center. Because the galactic center is located on the Southern hemisphere at right ascension (RA) 266.3° and declination (Dec) −29.0°,

the corresponding peak is not shown, but a large-scale anisotropy is clearly visible.

The differential neutrino flux is given by [11]

$$\frac{\mathrm{d}\phi_\nu}{\mathrm{d}E} = \frac{\langle\sigma_A v\rangle}{2} J_a(\psi) \frac{R_{\mathrm{SC}}\rho_{\mathrm{SC}}^2}{4\pi m_\chi^2} \frac{\mathrm{d}\mathscr{N}}{\mathrm{d}E}. \quad (3)$$

The factor $1/4\pi$ comes from isotropic emission of the final-state products and m_χ is the mass of the WIMP. $\frac{\mathrm{d}\mathscr{N}}{\mathrm{d}E}$ is the energy spectrum of final-state neutrinos, which is obtained by DarkSUSY [12] for benchmark WIMP masses and annihilation channels. $\langle\sigma_A v\rangle/2$ is the velocity-averaged self-annihilation cross-section per particle.

3 The IceCube Neutrino Observatory

IceCube is a Cherenkov neutrino detector located at the geographic South Pole [13]. Neutrinos interact with the clear Antarctic ice and produce secondary leptons and hadrons. These relativistic secondary particles produce Cherenkov light which is detected with Digital Optical Modules (DOMs). IceCube consists of 86 strings each instrumented with 60 DOMs, which are located at depths from 1.45 km to 2.45 km below the surface. The strings are arranged in a hexagonal pattern with an inter-string spacing of 125 m and a DOM-to-DOM distance of 17 m. A more densely instrumented sub-array called DeepCore, consisting of eight densely-instrumented strings, has been embedded to lowers the energy threshold from about 100 GeV to about 10 GeV [14]. The total instrumented volume is about one km^3. The detector construction was completed in December 2010.

4 Data Sample

This analysis uses data measured from June 2010 to May 2011, when IceCube was operating in its partial 79-string configuration. Within the live-time T_{live} of 316 days, 57281 up-going muon neutrinos from the Northern hemisphere were detected. We use muon events with reconstructed declinations of 0° to 90° to reduce the atmospheric muon contamination of the sample. By means of a mixture of straight cuts and a selection by a Boosted Decision Tree (BDT) [15] the atmospheric muon contamination was reduced to $< 3\%$ [16, 17]. The resulting sample consists mostly of atmospheric neutrinos, which are background for the search of neutrinos from self-annihilating dark matter in the galactic halo. Unlike signal, the integrated atmospheric neutrino flux is nearly constant as function of RA [18].

5 Analysis Method

To search for the anisotropy caused by an additional flux from WIMP annihilations in the Galactic Halo, we perform a multipole expansion of the neutrino arrival directions in equatorial coordinates. This is based on spherical harmonics

$$Y_\ell^m(\theta,\phi) = \sqrt{\frac{(2\ell+1)(\ell-m)!}{4\pi(\ell+m)!}} P_\ell^m(\cos(\theta)) \exp(\mathrm{i}m\phi) \quad (4)$$

where θ is the declination and ϕ is the right ascension. P_ℓ^m are the associated Legendre polynomials and build up the canonical solution of the Legendre equation with $-\ell \leq m \leq \ell$, where ℓ, m are separation constants [19]. Because spherical harmonics build a complete set of orthonormal functions on the full sphere Ω, all integrable functions $f(\theta,\phi)$ in the range $-\frac{\pi}{2} \leq \theta \leq \frac{\pi}{2}$ and $0 \leq \phi \leq 2\pi$ can be expanded in terms of spherical harmonics with the complex expansion coefficients

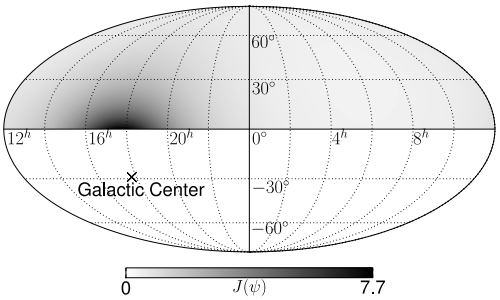

Figure 1: The dimensionless line-of-sight integral for the NFW model is shown for the northern hemisphere in equatorial coordinates. The anisotropy in the line-of-sight integral causes the anisotropy in the flux from self-annihilation of dark matter in the galactic halo. The position of the galactic center is indicated by the cross.

$$a_\ell^m = \int_\Omega \mathrm{d}\Omega\, f(\theta,\phi) Y_\ell^{m*}(\theta,\phi). \quad (5)$$

The expansion coefficients are calculated up to a maximal ℓ of $\ell_{\mathrm{max}} = 100$ using the software package HEALPix[1] [20]. The skymap is described by

$$f(\theta,\phi) = \sum_{i=1}^{N_\nu} \delta(\cos(\theta) - \cos(\theta_i)) \cdot \delta(\phi - \phi_i), \quad (6)$$

where (θ_i,ϕ_i) is the measured arrival direction of each neutrino, N_ν is the total number of neutrinos on the skymap and $\delta(x)$ is the Dirac delta distribution. To generate skymaps of arrival directions, atmospheric neutrinos and missreconstructed muons are simulated as background, where declinations are taken from experimental data and right ascensions are uniformly randomized. Neutrinos from WIMP annihilation in the Galactic Halo are generated taking into account the line-of-sight integral, the angular resolution and the detector acceptance. The number of events from WIMP annihilation is varied in simulation. The number of events per skymap is fixed to the total number of measured events in the experimental sample by adding the remaining number of events from the background simulation. In Fig. 2 and Fig. 3 the mean absolute value, also called power, of pure background and signal skymaps is shown. For background, nearly all power is contained in a_ℓ^0-coefficients, but for signal there is also power in coefficients with small m. The absolute value of the expansion coefficient is proportional to the signal strength, which can be found by simulation. In coefficients with large power there is also a preferred direction, indicated by the phase of the expansion coefficient. We combine phase and absolute value of the coefficient by projecting the complex expansion coefficient a_ℓ^m on the expected phase of the coefficient $a_{\ell,\mathrm{halo}}^m$ from pure signal skymaps. The resulting projection is given by

$$\mathscr{A}_\ell^m = \|a_\ell^m\| \cos\left(\arg(a_\ell^m) - \left\langle \arg\left(a_{\ell,\mathrm{halo}}^m\right)\right\rangle\right), \quad (7)$$

1. http://healpix.jpl.nasa.gov

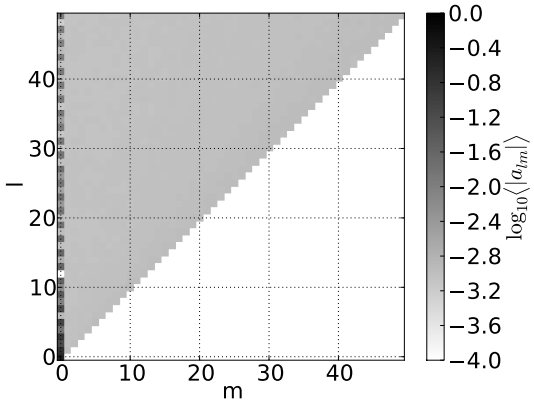

Figure 2: Shown is the logarithm of the absolute value for all coefficients in the ℓ-m-plane. The absolute value was averaged over 1000 pure background skymaps.

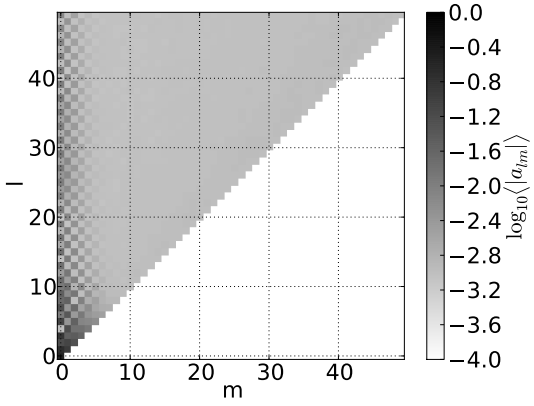

Figure 3: Shown is the logarithm of the absolute value for all coefficients in the ℓ-m-plane. The absolute value was averaged over 1000 pure signal skymaps.

where $\arg\left(a_\ell^m\right)$ gives the phase of the complex number a_ℓ^m. To separate signal from background, we define a test statistic based on the difference of $\mathscr{A}_\ell^m$ to the background estimation from atmospheric neutrinos $\mathscr{A}_{\ell,\mathrm{atm}}^m$. The test statistic is motivated by a weighted χ^2-function and is given by

$$D^2 = \frac{1}{\sum w_\ell^m} \sum_{\ell=1}^{\ell_{\max}} \sum_{m=1}^{\ell} \mathrm{sign}\left(\mathscr{A}_\ell^m\right) w_\ell^m \left(\frac{\mathscr{A}_\ell^m - \left\langle \mathscr{A}_{\ell,\mathrm{atm}}^m \right\rangle}{\sigma\left(\mathscr{A}_{\ell,\mathrm{atm}}^m\right)} \right)^2, \tag{8}$$

where $\langle x \rangle$ describes the mean and $\sigma(x)$ the standard deviation of the coefficients calculated from 1000 skymap simulations. The weights

$$w_\ell^m = \left\| \frac{\left\langle \mathscr{A}_{\ell,\mathrm{halo}}^m \right\rangle - \left\langle \mathscr{A}_{\ell,\mathrm{atm}}^m \right\rangle}{\sigma\left(\mathscr{A}_{\ell,\mathrm{atm}}^m\right)} \right\|, \tag{9}$$

are determined from pure halo signal skymaps. As can be seen from equation (4), spherical harmonics with $m = 0$ are independent of RA and just depend on declination. In the test statistic, the coefficients with $m = 0$ are excluded to reduce systematic uncertainties, which are dominated by uncertainties in the zenith dependent detector acceptance.

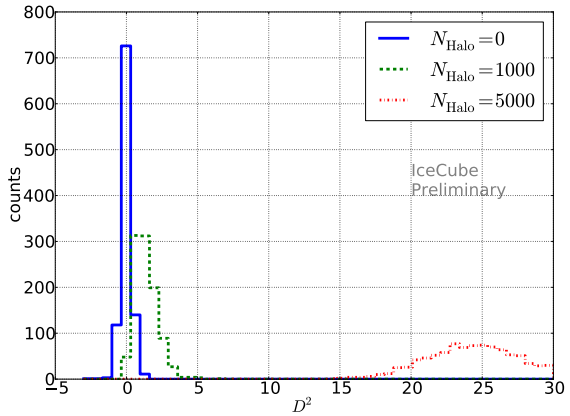

Figure 4: Test statistic D^2 for pure background simulation (solid) and simulations with small signal contributions. N_{halo} is the number of simulated neutrino arrival directions from WIMP annihilation in the Galactic Halo.

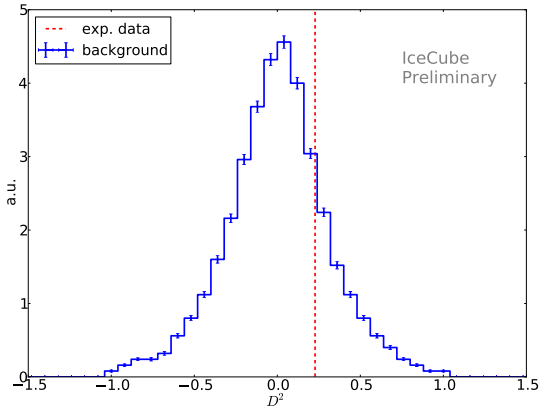

Figure 5: D^2-distribution for background expectation (solid) and the experimental observed value D^2_{exp} (dashed). The error of the background distribution reflects the simulation statistics.

The test statistic D^2 is plotted for pure background simulation and simulation with small signal contribution in Fig. 4. For each configuration 1000 skymaps were analyzed.

6 Results

The experimental value of the test statistic is $D^2_{\mathrm{exp}} = 0.23$. This corresponds to an overfluctuation of 0.79σ. The probability to observe this value or higher from background-only case is 22%. The background D^2-distribution and the measured D^2_{exp} value are shown in Fig. 5.

Based on the Feldman-Cousins approach [21], the 90% C.L. upper limit on the number of signal events has been calculated to $N_{90} = 1061$. This number can be converted to a limit on the velocity-averaged self-annihilation cross-section by

$$\langle \sigma_A v \rangle_{90} = \frac{8\pi m_\chi^2}{R_{\mathrm{SC}} \rho_{\mathrm{SC}}^2} \frac{1}{T_{\mathrm{live}}} \frac{1}{\int\int J(\psi) A_{\mathrm{eff}} \frac{\mathrm{d}\mathcal{N}_\nu}{\mathrm{d}E} \mathrm{d}E \mathrm{d}\Omega} N_{90}, \tag{10}$$

where T_{live} is the live-time and A_{eff} is the effective area of

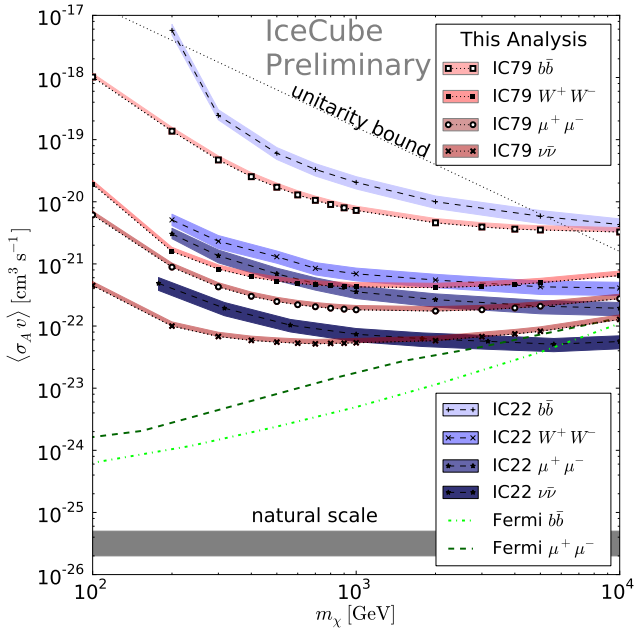

Figure 6: Upper limits on velocity-averaged WIMP self-annihilation cross-section from this analysis (IC79) and limits from halo analyses of IceCube-22 [18] (both 90% C.L.) and from the Fermi collaboration [22] (3σ C.L.). The limits from Fermi-LAT [22] are scaled by a factor of 2, to account for the different assumption on the local DM density of $0.43\,\mathrm{GeV/cm^3}$. The Fermi analysis region is $\pm 15^\circ$ in Galactic latitude, excluding the central $\pm 5^\circ$. The baseline limit curves are calculated for the NFW profile. The model-dependence (bands) has been estimated from two more extreme cases of a cusped, and a flat-cored halo model. The gray band describes the natural scale if all dark matter consists of WIMPs.

uncertainty	effect on $\langle\sigma_A v\rangle$
zenith acceptance	$< 1\%$
sky direction exposure	$\pm 1\%$
cosmic ray anisotropy	$\pm 3\%$
efficiency	$\pm 15\%$

Table 1: Systematic uncertainties

the detector, which includes the detection efficiency. The resulting limits for the benchmark annihilation channels $b\bar{b}$, W^+W^-, $\mu^+\mu^-$ and $\nu\bar{\nu}$ are shown in Fig. 6. For comparison the limits of halo analyses from IceCube-22 [18] and Fermi [22] are also shown.

7 Systematic Uncertainties

The presented limits depend on the assumed halo density model. We used the NFW halo model as a benchmark and compare to the profiles by Moore [9] and Burkert [10] (bands in Fig. 6). The model dependency of $+12\%/-1\%$ on $\langle\sigma_A v\rangle$ is much smaller than for galactic center searches, because typical differences in the halo models are smaller for the outer halo. Also the uncertainty is reduced with respect to the previous IceCube analyses.

Systematic uncertainties resulting from the analysis method itself are listed in Table 1. For a 5% flatter or steeper zenith acceptance spectrum the value of N_{90}, and therefore of $\langle\sigma_A v\rangle$, increases by less than 1%. This small dependency is a result of omitting coefficients which depend on declination. A systematic uncertainty of the order of 3% on N_{90} arises from a potential anisotropy of cosmic rays and the time-dependent exposure of the detector. A further systematic uncertainty is the effective area of the experiment. Our preliminary estimate based on the energy range of this analysis is $\pm 15\%$.

8 Conclusion

We present a search for self-annihilation of dark matter with the partially instrumented IceCube detector in its 79-string configuration based on a multipole expansion of the measured neutrino arrival directions. We search for a large-scale anisotropy in neutrino arrival directions from the Northern hemisphere, which corresponds to the outer Galactic Halo. The observed test statistic value is compatible with the null-hypothesis resulting in a limit on the velocity averaged self-annihilation cross-section for $\chi\chi \to b\bar{b}, W^+W^-, \mu^+\mu^-, \nu\bar{\nu}$ of the order of $10^{-18}\,\mathrm{cm^3/s}$ to $10^{-22}\,\mathrm{cm^3/s}$, assuming the NFW profile. Uncertainties in the detector acceptance have been largely reduced by obmitting expansion coefficients that depend on the zenith angle. Due to these smaller systematic uncertainties, as well as a larger detection efficiency the resulting sensitivity is stronger with respect to previous studies [18], especially in the low-mass region. However, due to the measured overfluctuation in this analysis the limits are about a factor two less constrained compared to the sensitivity.

References

[1] G. Bertone *et al.*, Phys. Rept. 405 (2005) 279.
[2] D. Larson *et al.*, Astrophys. J. Sup. 192 (2011) 16.
[3] P. A. R. Ade *et al.*, arXiv:1303.5076.
[4] G. Steigman *et al.*,Nucl. Phys. B 253 (1985).
[5] K. Griest *et al.*,Phys. Rev. Lett. 64 (1990).
[6] W. J. G. de Blok, Adv. Astron., 2010 (2010) 789293.
[7] L. Hernquist, Astrophys. J. 356 (1990) 359.
[8] J. F. Navarro *et al.*,Astrophys. J. 462 (1996) 563.
[9] B. Moore *et al.*, Mon. Not. Roy. Astron. Soc. 310 (1999) 1147.
[10] A. Burkert, Astrophys. J. Let. 447 (1995) 25.
[11] H. Yuksel *et al.*, Phys. Rev. D 76 (2007) 123506.
[12] P. Gondolo *et al.*, J. Cosmol. Astropart. Phys. 0407 (2004).
[13] A. Achterberg *et al.*, Astropart. Phys. 26 (2006) 155.
[14] R. Abbasi *et al.*, Astropart. Phys. 35 (2012) 615.
[15] S. S. Kerthi *et al.*, Neural Comp. 13 (2001) 637.
[16] M. G. Aartsen *et al.*, in preparation (2013).
[17] IceCube Coll., paper 0550 these proceedings.
[18] R. Abbasi *et al.*, Phys. Rev. D 84 (2011) 022004.
[19] J. D. Jackson, *Classical Electrodynamics*, Wiley, 3rd edition, (1998).
[20] K. M. Górski *et al.*, Astrophys. J. 622 (2005) 759.
[21] G. J. Feldman *et al.*,Phys. Rev. D 57 (1998) 3873.
[22] M. Ackermann *et al.*, Astrophys. J. 761 (2012) 91.